

MATERIAL POINT METHOD IN THREE-DIMENSIONAL PROBLEMS OF GRANULAR FLOW

ZDZISŁAW WIĘCKOWSKI* AND MICHAŁ PAWLAK†

*Łódź University of Technology, Department of Mechanics of Materials
al. Politechniki 6, 90-924 Łódź, Poland
e-mail: zwi@p.lodz.pl, web page: http://kmm.p.lodz.pl/staff/Z_Wieckowski

†Łódź University of Technology, Department of Mechanics of Materials
al. Politechniki 6, 90-924 Łódź, Poland
e-mail: michal.pawlak@p.lodz.pl, web page: http://kmm.p.lodz.pl/staff/M_Pawlak

Key words: material point method, finite element method, finite deformations, arbitrary Lagrangian–Eulerian description, granular flow

Abstract. The problem of flow of a granular material is considered in the paper. Dynamic, three-dimensional problems are analysed. As a tool of analysis, the material point method is utilized. The standard finite element method formulated in the Lagrangian description of motion appears to be not sufficiently robust in the analysis due to large distortions of the flowing granular material. The material point method is a variant of the finite element method which enables to solve the equations of motion on an arbitrary computational element mesh and trace state variables at points of the body chosen independently of the mesh. The material point method can be regarded as an arbitrary Lagrangian–Eulerian formulation of the finite element method. As all the state variables of the analysed body are traced at the points defined independently of an element mesh, the method can also be classified as a point-based (meshless) method. The mechanical behaviour of the granular material is described by the use of an elastic–viscoplastic material model.

1 INTRODUCTION

Three-dimensional gravitational flow problem of a granular material is considered. The dynamic, large strain problem still appears to be difficult in analysis although many well developed computational methods are available. For example, the standard finite element method formulated in the Lagrangian description of motion is not sufficiently robust for analysis of granular flow processes due to the problem of large mesh distortions which deteriorates the accuracy of the approximate solution. A mesh re-zoning technique aided to the Lagrangian approach is not a comprehensive remedy to overcome the problem as

it need mapping state variables from the distorted mesh to a newly generated one which is an additional source of computational inaccuracies. On the other hand, the use of an Eulerian formulation of the finite element method is disadvantageous because of inherent convective terms in equations of motion and troubles related to tracing free surfaces.

In the present work, the considered problem is solved by the use of the material point method (MPM), which is a variant of the finite element method formulated in an arbitrary Lagrangian–Eulerian description of motion (ALE). MPM is well known as a particle-in-cell method in fluid mechanics [1]. At the beginning of the last decade of the twentieth century, the method was adapted to problems of solid mechanics and called a material point method [2, 3].

The motion of so-called material (Lagrangian) points representing subregions of the analysed body is traced with respect to the background computational mesh which is of the Eulerian type. As the material points are defined independently of the computational mesh, MPM can be regarded as a point-based method. The method allows to analyse problems of very large strains [4].

2 SETTING OF THE PROBLEM

Let us consider a time interval $I = [0, T]$, where $T > 0$. Let $\Omega \subset \mathbb{R}^3$ denote the region occupied by the body at time $t \in I$, the boundary, $\partial\Omega$, of which consists of two parts Γ_u and Γ_σ such that

$$\overline{\Gamma_u} \cup \overline{\Gamma_\sigma} = \partial\Omega, \quad \Gamma_u \cap \Gamma_\sigma = \emptyset.$$

The solution to the problem satisfies the governing relations described in the subsections below.

2.1 Equations of motion

The equations of motion are as follows:

$$\sigma_{ij,j} + \rho b_i - \rho a_i = 0 \quad \text{on } \Omega, \tag{1}$$

where σ_{ij} denotes the Cauchy stress tensor, ρ is the mass density, b_i and a_i are vectors of body forces and acceleration, respectively.

2.2 Boundary conditions

It is assumed that the displacements are given on the boundary part Γ_u ,

$$u_i = U_i \quad \text{on } \Gamma_u,$$

and stresses are known on the part Γ_σ ,

$$\sigma_{ji} n_j = t_i \quad \text{on } \Gamma_\sigma$$

where t_i is the Cauchy stress vector, and n_i denotes the unit vector outwardly normal to the boundary $\partial\Omega$.

2.3 Initial conditions

The following initial conditions are considered:

$$u_i(0) = u_i^0, \quad \dot{u}_i(0) = v_i^0, \quad \sigma_{ij}(0) = \sigma_{ij}^0, \quad (2)$$

where u_i^0 , v_i^0 and σ_{ij}^0 denotes the initial fields of displacements, velocities and stresses, respectively.

2.4 Constitutive relations

An elastic–viscoplastic constitutive model with the Drucker–Prager yield condition and a non-associated flow rule is utilized to describe mechanical behaviour of the granular material. The yield function has the form:

$$f(\sigma_{ij}) = q - m p \quad (3)$$

where parameter $m = 18 \sin \varphi / (9 - \sin^2 \varphi)$ depends on the angle of internal friction, φ , p and q are stress invariants defined as follows:

$$p = -\frac{1}{3} \sigma_{ii}, \quad q = \sqrt{\frac{3}{2} s_{ij} s_{ij}} \quad (4)$$

where $s_{ij} \equiv \sigma_{ij} + p \delta_{ij}$ denotes the deviatoric part of the stress tensor.

After defining the deviatoric part of the rate-of-deformation tensor, d_{ij} , $e_{ij} = d_{ij} - \frac{1}{3} d_{kk} \delta_{ij}$, the constitutive relations can be written in the form

$$\begin{aligned} \dot{p} &= -K d_{kk}, \\ e_{ij} &= e_{ij}^e + e_{ij}^{\text{vp}}, \\ e_{ij}^e &= \frac{1}{G} \overset{\nabla}{s}_{ij}, \\ e_{ij}^{\text{vp}} &= \gamma \langle \Phi(f) \rangle \frac{\partial g}{\partial s_{ij}} \end{aligned} \quad (5)$$

where e_{ij}^e and e_{ij}^{vp} are the elastic and viscoplastic parts of tensor e_{ij} , K denotes the bulk modulus, G the shear modulus, γ the viscosity parameter and g the plastic potential defined by the relation $g = q$, which means that the material is plastically incompressible. Symbol $\overset{\nabla}{s}_{ij}$ denotes the Jaumann stress rate tensor defined as follows:

$$\overset{\nabla}{\sigma}_{ij} = \sigma_{ij} - \sigma_{ik} \omega_{kj} - \sigma_{jk} \omega_{ki} \quad (6)$$

where ω_{ij} is the spin tensor. Function Φ is defined as follows:

$$\Phi(f(\sigma_{ij})) = \left(\frac{q - m p}{m p} \right)^N, \quad N > 0, \quad (7)$$

an idea proposed by Perzyna [5] is utilized here.

The bulk and shear moduli used in the above equations can be expressed by the Young modulus, E , and Poisson ratio, ν ,

$$K = \frac{E}{3(1-2\nu)}, \quad G = \frac{E}{2(1+\nu)}. \quad (8)$$

3 MATERIAL POINT SOLUTION OF THE PROBLEM

3.1 Variational formulation of the problem

The material point method is based on the variational formulation of governing relations as the finite element method. Using the principle of virtual work, the problem can be stated in the form of the following equation:

$$\forall \delta \mathbf{u} \in V_0 \quad \int_{\Omega} \varrho \left(a_i \delta u_i + \frac{1}{\varrho} \sigma_{ij} \delta u_{i,j} \right) dx = \int_{\Omega} \varrho b_i \delta u_i dx + \int_{\Gamma_\sigma} t_i \delta u_i ds \quad (9)$$

where V_0 is the space of kinematically admissible displacement fields satisfying the homogeneous boundary conditions.

3.2 Space discretization

Two kinds of space discretization are used in the material point method. Firstly, the initial configuration of the analysed body is divided into a finite number of subregions. Each of these subregions is represented by one of its points, called a material point. Assuming that the whole mass of each subregion of the body is concentrated at the corresponding material point, the field of mass density can be expressed by masses of the material points and Dirac's δ -function as follows:

$$\varrho(\mathbf{x}) = \sum_{P=1}^N M_P \delta(\mathbf{x} - \mathbf{X}_P) \quad (10)$$

where M_P and \mathbf{X}_P denote the mass and position of the P th material point, respectively.

On the other hand, a finite element mesh of an Eulerian type is introduced for approximation of unknown kinematic fields. Using the finite element interpolation technique for the acceleration and displacement fields $\mathbf{a} = \mathbf{N} \mathbf{a}$, $\mathbf{u} = \mathbf{N} \mathbf{u}$, Eqn. (9) can be written in the form

$$\delta \mathbf{u}^T \left(\sum_{P=1}^N \left[M_P \mathbf{N}_P^T \mathbf{N}_P \mathbf{a} + M_P \mathbf{B}_P^T \frac{\boldsymbol{\sigma}}{\varrho}(\mathbf{X}_P) - M_P \mathbf{N}_P^T \mathbf{b}(\mathbf{X}_P) \right] - \int_{\Gamma_\sigma} \mathbf{N}^T \mathbf{t} ds \right) = 0 \quad (11)$$

where \mathbf{N}_P and \mathbf{B}_P denote the matrix of shape functions and the strain-displacement matrix, respectively, calculated at the point \mathbf{X}_P . Eqn. (11) leads to the system of dynamic equations,

$$\mathbf{M} \mathbf{a} = \mathbf{F} - \mathbf{R} \quad (12)$$

where \mathbf{M} is the mass matrix, \mathbf{F} and \mathbf{R} denote the vectors of nodal external and internal forces, respectively, defined as follows:

$$\begin{aligned} \mathbf{M} &= \sum_{P=1}^N M_P \mathbf{N}_P^T \mathbf{N}_P, \\ \mathbf{F} &= \sum_{P=1}^N M_P \mathbf{N}_P^T \mathbf{b}(\mathbf{X}_P) + \int_{\Gamma_\sigma} \mathbf{N}^T \mathbf{t} \, ds, \\ \mathbf{R} &= \sum_{P=1}^N M_P \mathbf{B}_P^T \end{aligned} \quad (13)$$

where N is the number of material points, $\mathbf{N}_P \equiv \mathbf{N}(\mathbf{X}_P)$, and \mathbf{B} denotes the strain-displacement matrix containing the derivatives of the interpolation functions.

3.3 Time integration of dynamic problem

The solution to the dynamic system (12) is found for a discrete set of instants $t_1, t_2, \dots, t, t + \Delta t, \dots \in I$ ($I \equiv [0, T], 0 < t_1 < t_2 < \dots < t < t + \Delta t < \dots < T$). Using the explicit time integration procedure, the vector of nodal accelerations, $\mathbf{a}^{t+\Delta t}$, is calculated by solving the system of equations

$$\mathbf{M}^t \mathbf{a}^{t+\Delta t} = \mathbf{F}^t - \mathbf{R}^t, \quad (14)$$

and the vector of nodal velocities, $\mathbf{v}^{t+\Delta t}$, from the relation

$$\mathbf{v}^{t+\Delta t} = \mathbf{v}^t + \Delta t \mathbf{a}^{t+\Delta t}. \quad (15)$$

Each time increment consists of two steps: the Lagrangian step and the convective one. In the Lagrangian step, the calculations are performed in a similar way as in the updated Lagrangian formulation of the standard finite element method; it is assumed that the computational mesh deforms together with the considered body. The kinematic state variables are calculated for each material point by the use of the interpolation functions and nodal parameters defined on the computational mesh. Particularly, the velocity vector for the P th material point, $\mathbf{V}_P \equiv [V_{Px} \ V_{Py} \ V_{Pz}]^T$, is obtained from the equation

$$\mathbf{V}_P = \mathbf{N}(\mathbf{X}_P) \mathbf{v}^e, \quad (16)$$

where $\mathbf{v}^e = [v_{1x} \ v_{1y} \ v_{1z} \ v_{2x} \ v_{2y} \ v_{2z} \ \dots \ v_{n_{ex}} \ v_{n_{ey}} \ v_{n_{ez}}]^T$ is the vector of the nodal velocities of the element which the material point belongs to. The vector of strain increment can be calculated using matrix \mathbf{B} as follows:

$$\Delta \mathbf{e} = \Delta t \mathbf{B}(\mathbf{X}_P) \mathbf{v}^e, \quad (17)$$

where $\Delta \mathbf{e} = \Delta t [d_{xx} \ d_{yy} \ d_{zz} \ d_{xy} \ d_{yz} \ d_{zx}]^T$. Then, stresses can be obtained from the constitutive relations. The backward Euler time integration procedure is utilized for the constitutive relations in this paper. The detailed description of the procedure is given in [4].

The convective step consists in mapping the velocity field from the material points to the nodes of the computational mesh. The mesh can be changed arbitrarily or remain in the same position as defined at the beginning of the time increment. The vector of nodal velocities

$$\mathbf{v} = [v_{1x} \ v_{1y} \ v_{1z} \ v_{2x} \ v_{2y} \ v_{2z} \ \dots \ v_{nx} \ v_{ny} \ v_{nz}]^T, \quad (18)$$

is calculated by solving the following least square problem

$$\sum_{P=1}^N M_P [\mathbf{N}(\mathbf{X}_P) \mathbf{v} - \mathbf{V}_P]^T [\mathbf{N}(\mathbf{X}_P) \mathbf{v} - \mathbf{V}_P] = \min \quad (19)$$

where masses of the material points play roles of weights. The vector of nodal velocities minimizing the above function is the solution to the following set of equations [2, 3]

$$\mathbf{M} \mathbf{v} = \mathbf{S}^T \mathbf{M}_d \mathbf{V} \quad (20)$$

which expresses equivalence of momentum calculated for the material points and for the computational grid, where $\mathbf{V} = [V_{1x} \ V_{1y} \ V_{1z} \ V_{2x} \ V_{2y} \ V_{2z} \ \dots \ V_{Nx} \ V_{Ny} \ V_{Nz}]^T$ is the vector of velocities of all the material points, and matrices \mathbf{S} and \mathbf{M}_d are defined as follows:

$$\mathbf{S} = \begin{bmatrix} \mathbf{N}(\mathbf{X}_1) \\ \mathbf{N}(\mathbf{X}_2) \\ \vdots \\ \mathbf{N}(\mathbf{X}_N) \end{bmatrix}, \quad \mathbf{M}_d = \begin{bmatrix} \mathbf{M}_1 & \mathbf{0} & \dots & \mathbf{0} \\ \mathbf{0} & \mathbf{M}_2 & \dots & \mathbf{0} \\ \vdots & \vdots & \ddots & \vdots \\ \mathbf{0} & \mathbf{0} & \dots & \mathbf{M}_N \end{bmatrix}, \quad \mathbf{M}_i = \begin{bmatrix} M_i & 0 & 0 \\ 0 & M_i & 0 \\ 0 & 0 & M_i \end{bmatrix}. \quad (21)$$

Because of the Dirac delta function representation of mass density, the mass matrix \mathbf{M} is singular when consistent form is considered in the case of triangular elements with the linear shape functions. To solve system (12), the diagonalized matrix, \mathbf{M}_l , or nearly consistent matrix $\mathbf{M}_\alpha = \alpha \mathbf{M} + (1 + \alpha) \mathbf{M}_l$, can be used instead of \mathbf{M} , where $0 \leq \alpha \leq 1$ (see e.g. [2]).

All the details of solution of the system (11) can be found in References [3] and [4].

4 EXAMPLE: COLLAPSING WALL PROBLEM

The motion of a collapsing sand wall is considered in this Section. The wall has dimensions $2\text{ m} \times 2\text{ m}$ in the xz -plane and is infinitely long in the y -direction (Figure 1). The elastic–viscoplastic constitutive model presented in Section 2.4 is utilized in the

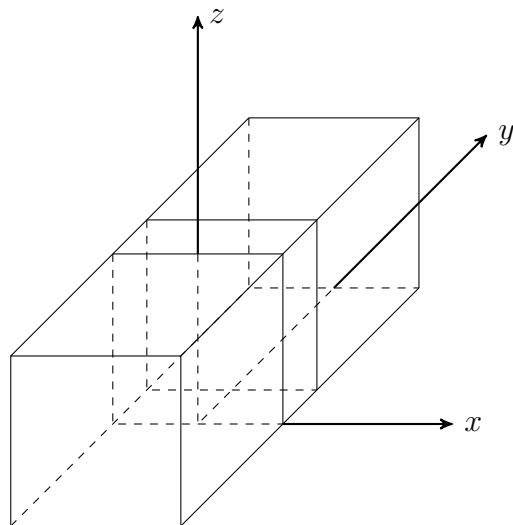


Figure 1: Collapsing wall problem

analysis. Calculations have been made with the following material data: mass density $\rho = 1500\text{ kg/m}^3$, the angle of internal friction $\varphi = 30^\circ$, Young’s modulus $E = 1 \cdot 10^6\text{ Pa}$, Poisson’s ratio $\nu = 0.3$, viscosity coefficient $\gamma = 50\text{ s}^{-1}$, exponent in the viscoplastic law $N = 1$.

It is assumed that the considered granular body does not move at time $t = 0$ and the initial stress field has the following components:

$$\begin{aligned}\sigma_{zz} &\equiv \sigma_{zz}(z) = -\rho g (h - z), \\ \sigma_{xx} = \sigma_{yy} &= 0.3 \sigma_{zz}, \\ \sigma_{xy} = \sigma_{yz} = \sigma_{zx} &= 0\end{aligned}\tag{22}$$

where $h = 2\text{ m}$ denotes the height of the wall.

The plane motion of the wall is studied by means of the three-dimensional analysis; a thin slice with the thickness of 0.2 m —shown in Figure 1—is considered and the y -component of the displacement field is equal to zero for the two vertical planes bounding the slice.

Owing to the symmetry of the problem, one half of the slice has been discretised (for $x \geq 0$). The mesh consisting of 10565 nodes and 50743 tetrahedral elements with linear interpolation functions has been used in the calculations. The region representing the granular material has been discretised by 1600 material points. The time increment used

in the calculations has been set as follows: $\Delta t = 5 \cdot 10^{-5}$ s. Several stages of deformation of collapsing wall is shown in Figure 2. The results of the three-dimensional computations (figures in the right column) are compared with those obtained by the use of the two-dimensional analysis (figures in the left column). The similarity of the results is noticed; the pattern and rate of deformation look similar.

At the end of the deformation process the granular material reaches the equilibrium, approximately after 2 s. The position of the granular material at this time instant obtained in the three-dimensional analysis and shown in a perspective view is given in Figure 3. Outlines of the computational meshes used in the calculations are shown in Figures 2 and 3.

5 CONCLUSIONS

A three-dimensional implementation of the material point method is presented in the paper and applied to a problem of granular flow. The approach allows one to solve such a problem despite the very large strains observed in the case of deformation of the granular media. Four-node tetrahedral elements have been used in defining the computational mesh which allows for description of an arbitrary geometry of a problem. An elastic–viscoplastic constitutive model has been utilized to describe the behaviour of the granular material. The results related to a problem of collapsing sand wall are presented. They have been compared with those obtained by the use of the two-dimensional material point model. Good agreement between both the results has been obtained. The presented example shows that the method can be applied to other challenging engineering tasks involving large distortions. Analyses of such problems like silo flows, landslides and motion of avalanches are planned.

ACKNOWLEDGMENTS

The financial support by IACM is gratefully acknowledged by the second author of the paper.

REFERENCES

- [1] Harlow, F.H. *The particle-in-cell computing method for fluid dynamics*. Methods for Computational Physics, Adler, B., Fernbach, S. and Rotenberg, M., Eds., Academic Press, New York, Vol. 3, pp. 319–343, 1964.
- [2] Burgess, D., Sulsky, D. and Brackbill, J.U., *Mass matrix formulation of the FLIP particle-in-cell method*. Journal of Computational Physics, 103, pp. 1–15, 1992.
- [3] Sulsky, D. and Schreyer, H.L., *Axisymmetric form of the material point method with applications to upsetting and Taylor impact problems*. Comput. Methods Appl. Mech. Engng., 139, pp. 409–429, 1996.

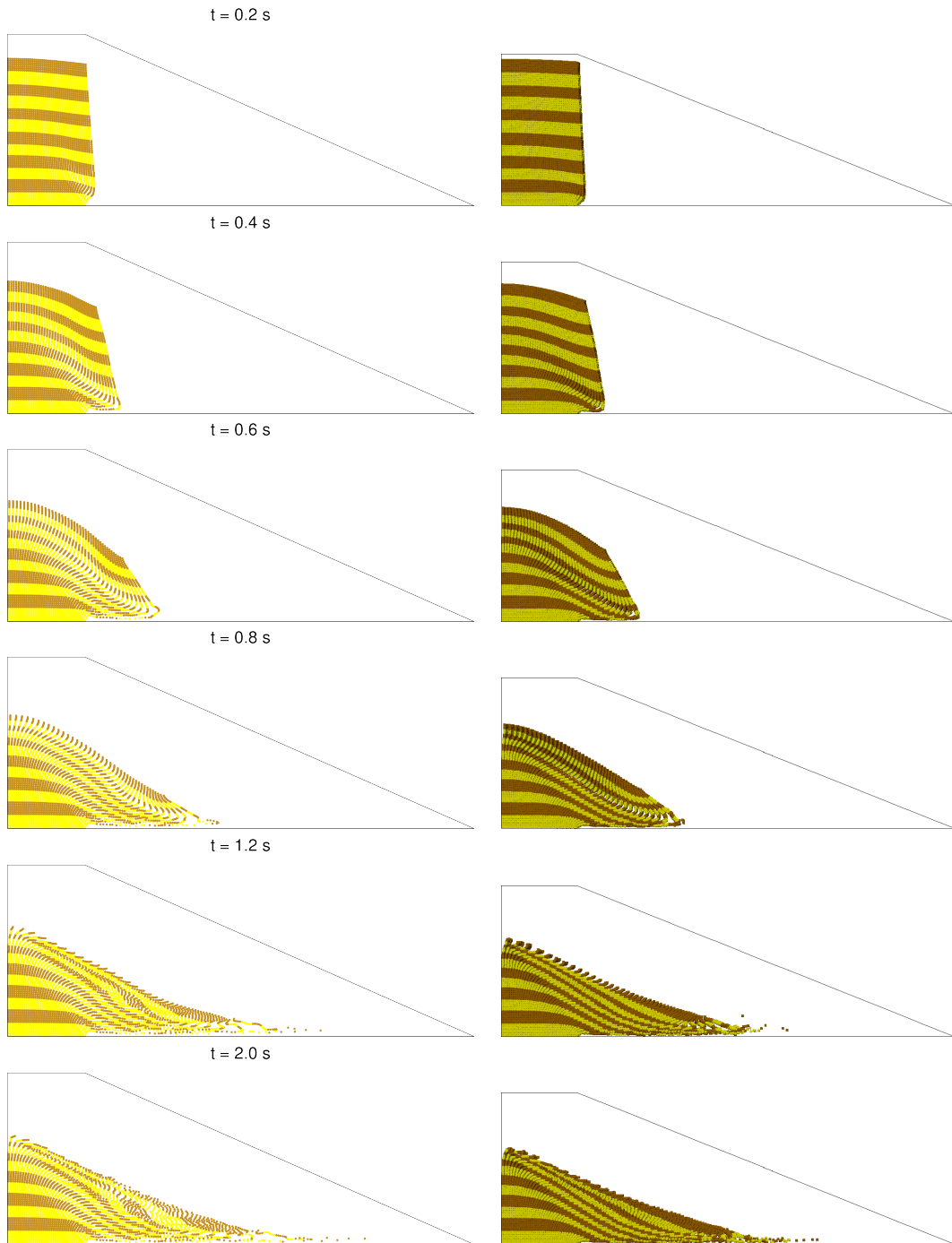


Figure 2: Several phases of the deformation process (on the left – two-dimensional solution, on the right – three-dimensional solution)

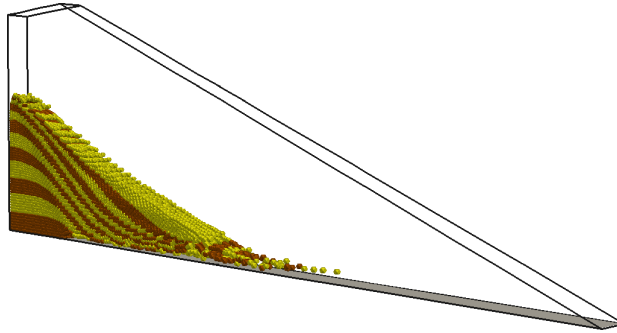


Figure 3: Final (equilibrium) stage calculated in 3D analysis

- [4] Więckowski, Z., *The material point method in large strain engineering problems*. Comput. Methods Appl. Mech. Engng., 193, pp. 4417–4438, 2004.
- [5] Perzyna, P., *Fundamental problems in visco-plasticity*, Adv. Appl. Mech., 9, pp. 243–377, 1966.